Sequential combinations of chemotherapeutic agents with BH3 mimetics to treat rhabdomyosarcoma and avoid resistance.

Clara Alcon[1], Albert Manzano-Muñoz[1], Estela Prada[2,3], Jaume Mora[2,3], Aroa Soriano[4], Gabriela Guillén[4,5], Josep Roma[4], Josep Samitier[1,6,7], Alberto Villanueva[8,9], Joan Montero[1,*].

1. Institute for Bioengineering of Catalonia (IBEC), Barcelona Institute of Science and Technology (BIST), 08028 Barcelona, Spain.

2. Developmental Tumor Biology Laboratory, Institut de Recerca Sant Joan de Déu, 08950 Esplugues de Llobregat, Spain.

3. Department of Haematology and Oncology, Hospital Sant Joan de Déu Barcelona, 08950 Esplugues de Llobregat, Spain

4. Group of Translational Research in Child and Adolescent Cancer, Vall d'Hebron Research Institute (VHIR), Universitat Autònoma de Barcelona (UAB), 08035 Barcelona, Spain.

5. Department of Surgery, Universitat Autònoma de Barcelona (UAB), 08193. Barcelona, Spain.

6. Department of Electronics and Biomedical Engineering, University of Barcelona (UB), 08028 Barcelona, Spain.

7. Networking Biomedical Research Center in Bioengineering, Biomaterials and Nanomedicine (CIBER-BBN), 28029 Madrid, Spain.

8. Program against Cancer Therapeutic Resistance (ProCURE), IDIBELL, Catalan Institute of Oncology, 08907 l'Hospitalet del Llobregat, Barcelona, Spain.

9. Xenopat S.L., Business Bioincubator, Bellvitge Health Science Campus, 08907 l'Hospitalet de Llobregat, Barcelona, Spain

* Correspondance to Joan Montero (jmontero@ibecbarcelona.eu)

Institute for Bioengineering of Catalonia (IBEC), The Barcelona Institute of Science and Technology (BIST), Barcelona, Spain. Phone: +34 934 039 956; Fax: +34 934 039 702

Alcon et al

Abstract

Rhabdomyosarcoma (RMS) is the most common soft tissue sarcoma in childhood and adolescence. Refractory/relapsed RMS patients present a bad prognosis, that combined with the lack of specific biomarkers difficult the development of new therapies. We here utilize dynamic BH3 Profiling (DBP), a functional predictive biomarker that measures net changes in mitochondrial apoptotic signaling, to identify anti-apoptotic adaptations upon treatment. We use this information to guide the use of BH3 mimetics to specifically inhibit BCL-2 pro-survival proteins, defeat resistance and avoid relapse to therapy. Indeed, we found that BH3 mimetics that selectively target BCL-xL and MCL-1 synergistically enhance the effect of the clinically used chemotherapeutic agents vincristine and doxorubicin in RMS cells. We validated this strategy *in vivo* using a RMS patient-derived xenograft (PDX) model and observed a reduction on tumor growth with a tendency to its stabilization with the sequential combination of vincristine and the MCL-1 inhibitor S63845. Finally, we identified the molecular mechanism by which RMS cells acquire resistance to vincristine: through the anti-apoptotic protein MCL-1 for which we observed an enhanced binding between MCL-1 and BID after drug exposure. In conclusion, our findings validate the use of DBP as a functional assay to predict treatment effectiveness in RMS and provide a rationale for BH3 mimetic combination with chemotherapeutic agents to avoid tumor resistance, improve treatment efficiency and decrease undesired secondary effects.

Introduction

Rhabdomyosarcoma (RMS) is a highly malignant cancer that, despite being relatively rare, is the most frequent soft-tissue sarcoma in children, accounting for 5% of all pediatric tumors[1].

Alcon et al

RMS are highly aggressive tumors that typically develop from skeletal muscle cells and can arise in a variety of anatomic sites in the body[2,3]. There is a slightly higher prevalence of this disease in males than in females, and it is often associated with genetic disorders such as Li-Fraumeni familiar cancer syndrome and neurofibromatosis type 1[2]. Based on histologic criteria, RMS tumors are subdivided in two main groups, embryonal (ERMS) and alveolar (ARMS). ERMS account for 60% of all RMS, affecting children under the age of 10, especially around the head and neck region [2,3]. ARMS represent approximately 20% of all RMS, occurring mostly in adolescents, frequently localized in the limbs[3,4]. The current treatment strategies for RMS include chemotherapy, radiation, and surgery[4]. Despite treatment improvement for patients with low- and intermediate-risk disease, the survival rates for patients with high-risk disease has not advanced in the last decades[4]. Furthermore, the derived toxicity from current treatments and the lack of biomarkers[5] highlight the need for new therapies to enhance RMS clinical outcomes.

Therapy causes cancer cells' death mostly by apoptosis, a process controlled by the BCL-2 family of proteins[6]. This family members are classified based on their structure, BCL-2 homology (BH) domains and their function[6,7]. In brief, the anti-apoptotic proteins (BCL-2, BCL-xL MCL-1 and others) have four BH domains (BH1-BH4) and bind to pro-apoptotic proteins. The pro-apoptotic effector proteins BAX and BAK also contain four BH domains and have the capacity to oligomerize and form pores in the mitochondrial outer membrane. Their function is induced by activator proteins possessing a unique BH3 domain, such as BIM, BID, or PUMA. There is a fourth group of BCL-2 family proteins, the so-called sensitizers, also presenting a unique BH3 domain, that cannot directly activate effector proteins. Sensitizers include BAD, HRK, BIK, NOXA and BMF, among others, and exert a pro-apoptotic effect by competing for specific binding to anti-apoptotic BCL-2 family members[7]. Overall, these proteins regulate mitochondrial outer membrane permeabilization (MOMP) and release of

cytochrome c (and other proteins) that represents the point of no return for apoptotic cell death. Importantly, MOMP can be prevented by anti-apoptotic proteins through direct binding to BAX and BAK or activator BH3-only proteins[7].

Evasion of apoptosis is a hallmark of human cancers and it is often explained by anti-apoptotic proteins' increased expression[8,9]. In fact, high levels of BCL-2 and MCL-1 have been reported in RMS patients as a pro-survival mechanism[10,11]. Therefore, targeting anti-apoptotic proteins represents a promising therapeutic approach to treat high-risk or relapsed RMS patients[9,12]. In this regard, BH3 mimetics, a novel class of therapeutics that mimic the action of sensitizer BH3-only proteins to selectively inhibit anti-apoptotic BCL-2 family members[7], could be used to overcome apoptotic resistance. There is an increasing interest on BH3 mimetics for their therapeutic potential alone or in combination with other treatments, but the main question that clinicians will have to face is: when and how to use BH3 mimetics as anti-cancer therapies in the clinic[7]. On this subject, the functional assay dynamic BH3 profiling (DBP) can determine in less than 24 hours how effective a treatment will be to engage apoptosis[13]. Briefly, this technology uses synthetic BH3 peptides derived from BCL-2 family proteins to measure how close cells are to the apoptotic threshold – or how primed cells are for death. DBP has been successfully used to predict, days to weeks in advance, treatment effectiveness in cell lines, murine models and on patient samples[13–17]. In addition to overall susceptibility to apoptosis, DBP can identify cancer cells' selective dependence on anti-apoptotic proteins and guide BH3 mimetic use to overcome therapy-induced resistance[7].

Several publications by Fulda and colleagues elegantly demonstrate BH3 mimetics' therapeutic potential to treat RMS [12,18–20] although sequential combination of anti-cancer agents with BH3 mimetics has not been fully assessed. Here we report a new strategy that utilizes low-dose combinations of chemotherapeutic agents with BH3 mimetics to increase current treatments' efficacy while decreasing therapy-induced toxicity [21] and anti-apoptotic protection.

Alcon et al

Results

Novel chemotherapy combinations with BH3 mimetics to increase RMS cytotoxicity

Chemotherapeutic agents are commonly used in clinical protocols for RMS treatment[4]. However, they negatively impact patients with short- and long-term therapy toxicities[22], and often treatment resistance is acquired by cancer cells[23]. Therefore, we focused on reducing chemotherapeutic dosage to decrease therapy-associated undesired effects. First, we used DBP to analyze the increase in priming after incubation with four standard of care RMS chemotherapeutic agents: the microtubule destabilizing agent vincristine, the alkylating molecule cyclophosphamide, the anthracycline antibiotic with antineoplastic activity doxorubicin and the topoisomerase inhibitor etoposide[24]. We performed DBP on three different RMS cell lines to account for the disease heterogeneity: two ARMS cell lines (CW9019 and RH4) and an ERMS cell line (RD). We observed an increase in priming upon treatment (Δ% priming) after a short incubation with vincristine and doxorubicin, but not with cyclophosphamide or etoposide (Figure 1A and 1C). Using Annexin V and propidium iodide (PI) staining, we analyzed by flow cytometry cell death after 96 hours of exposure to the same chemotherapeutic agents as a proof of principle to evaluate the correlation between DBP predictions and later cell death. We observed high levels of cell death (between 40% and 80%) after vincristine treatment and even nearly complete elimination of cells with doxorubicin, but no effect with cyclophosphamide or etoposide, confirming DBP predictions (Figure 1B). We observed a similar trend in the two other RMS cell lines, RD and RH4 (Figure 1D). When we statistically compared Δ% priming and % cell death in all three cell lines, we observed a significant correlation between both measurements (Figure 1E. left). To determine how good DBP is as a binary predictor for RMS, we performed a receiver operating characteristic (ROC) curve analysis[25]. In our experiments the area under the curve (AUC) was 0.81 (Figure 1E.

Alcon et al

right), indicating that DBP presents a good predictive capacity for chemotherapy cytotoxicity
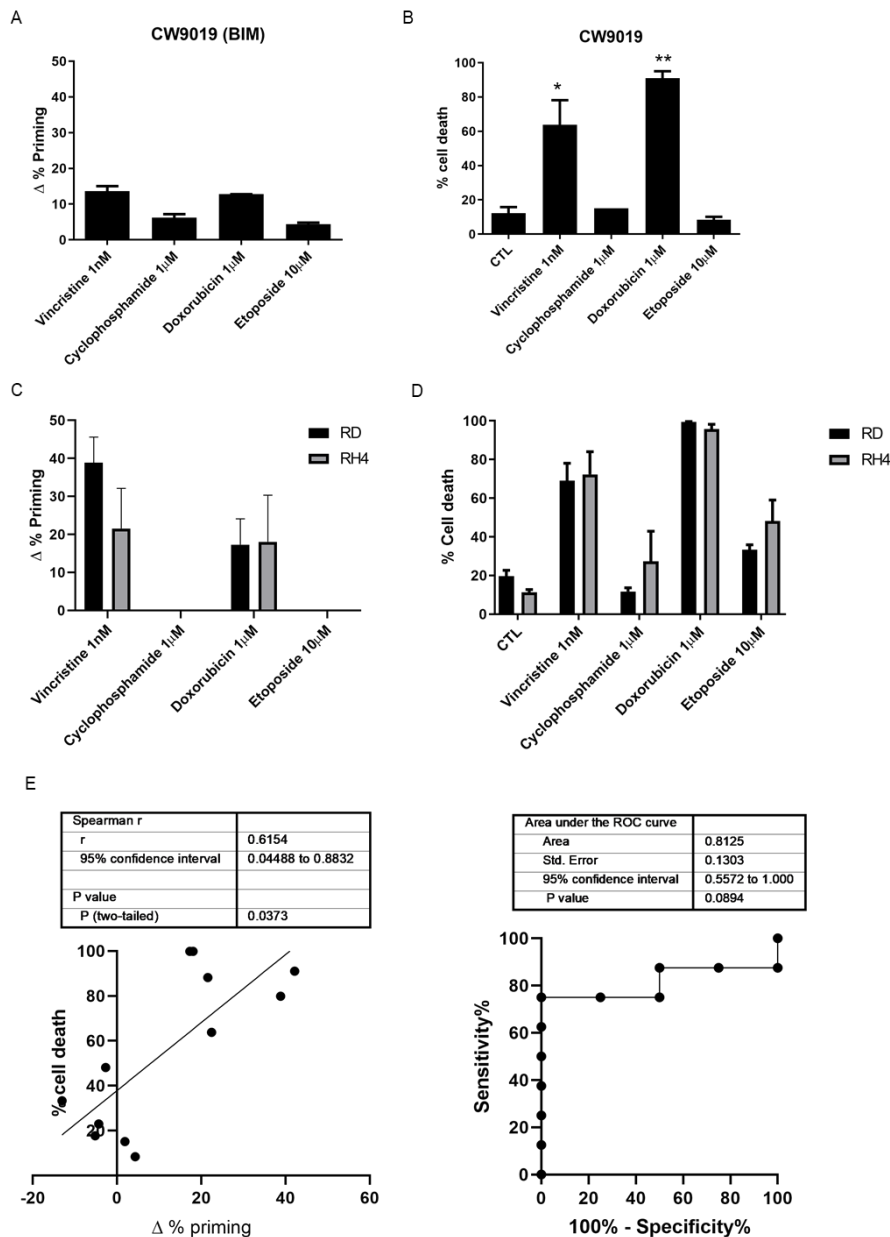
in all RMS cell lines tested.

Figure 1: Dynamic BH3 profiling predicts chemotherapy sensitivity in different RMS cell lines. *(A) Results from the DBP assay after 36 hours incubation with the treatments in CW9019 cells. Results expressed as Δ% priming represents the increase in priming compared to control cells. (B) Cell death results from Annexin V and propidium iodide staining and FACS analysis after 96 hours incubation with the chemotherapeutic agents in CW9019 cells. (C) Results from the DBP assay after 36 hours incubation with the treatments in RD and RH4 cells. Results expressed as Δ% priming represents the increase in priming compared to control cells. (D) Cell death results from Annexin V and propidium iodide staining and FACS analysis after 96 hours incubation with the chemotherapeutic agents in RD and RH4 cells. (E) Left plot showing the correlation between Δ% priming at 36 hours and % cell death at 96h. Receiver Operating Characteristic curve analysis showed at right. Values indicate mean values ± SEM from at least three independent experiments. ** p<0.01 and * p<0.05.*

6

As mentioned above, one of the hallmarks of cancer is treatment adaptation and resistance to anti-cancer drugs[23]. This resistance can be acquired by different mechanisms such as drug target alterations (mutations), drug export transporters' gain, increased DNA damage repair, altered proliferation and, as we further explored, through anti-apoptotic BCL-2 proteins[26]. Using specific synthetic BH3 peptides, that mimic sensitizer BCL-2 family proteins, with DBP we can identify what is anti-apoptotic protein that cancer cells depend on to become resistant to a given treatment[7]. In this regard, we can precisely evaluate the contribution of three main pro-survival BCL-2 family members: BCL-2/BCL-xL dependence with the BAD BH3 peptide, BCL-xL dependence with the HRK BH3 peptide and MCL-1 dependence with the MS1 BH3 peptide[7,27–30], after treating the cells with a specific therapeutic agent. Using this strategy, we identified in CW9019 cells that upon vincristine treatment an increase in Δ% priming with BAD, HRK and MS1 (Figure 2A), indicating that cancer cells acquire resistance to this agent mostly through BCL-xL and MCL-1. In consequence, we decided to pharmacologically exploit this dependence utilizing two new selective BH3 mimetics: S63845 (MCL-1 inhibitor) and A-1331852 (BCL-xL inhibitor) and test their cytotoxic effect in combination with vincristine. We observed that sequentially adding S63845 or A-1331852 after 16 hours of exposure to vincristine significantly increased cell death at 96 hours compared to single agents (Figure 2B). In fact, combination index (CI) calculations[31] indicated that S63845 addition to vincristine is synergistic (CI<1) while A-1331852 is additive (CI=1). Obtaining a synergistic combination between two agents is an important goal to decrease treatment toxicity and to avoid undesired side effects associated with high doses of chemotherapy, a constant challenge in pediatric cancer research[32]. We repeated these experiments with another RMS standard chemotherapeutic agent, doxorubicin, and we observed an increase in Δ% priming with DBP (Figure 1A) and a high percentage of cell death with Annexin V and propidium iodide staining

Alcon et al

(Figure 1B). Like vincristine, we could detect an increase in priming with BAD, HRK and MS1 in CW9019 cells (Figure 2C) indicating that cancer cells also acquired resistance to doxorubicin treatment through BCL-xL and MCL-1. Doxorubicin is already a potent chemotherapeutic agent as a single agent and exerts an extensive cytotoxicity after 96 hours (Figure 1B), but also causes cardiotoxicity in the clinic[21]. Therefore, we sought to reduce doxorubicin dosing by exploring synergistic sequences with the anti-apoptotic inhibitors A-1331852 and S63845. Hereof, doxorubicin combined with both BH3 mimetics was highly cytotoxic at 96 hours for RMS cells, even when reducing ten-fold its concentration (Figure 2D). Both combinations of doxorubicin with S63845 or A-1331852 are synergistic, as we observed a CI < 1. Additionally, we analyzed several BCL-2 family proteins expression to determine molecular fluctuations after vincristine and doxorubicin treatments. Surprisingly, we found that upon vincristine treatment there were no changes in anti-apoptotic proteins MCL-1, BCL-xL or BCL-2 expression, indicating that cancer cells' adaptation to this treatment relies on different mechanisms (Supplementary Figure 1). On the other hand, doxorubicin treatment lead to a marked decline in MCL-1 and BCL-xL levels, an increase in BCL-2 expression and a decrease in pro-apoptotic proteins BAK and BID (Supplementary Figure 1). From this first set of experiments we conclude that we can increase chemotherapeutic agents' cytotoxicity by combining them with specific BH3 mimetics. Particularly, sequential vincristine treatment followed by S63845 stands out as the most effective therapy *in vitro* for CW9019 RMS cells (Figure 2B).
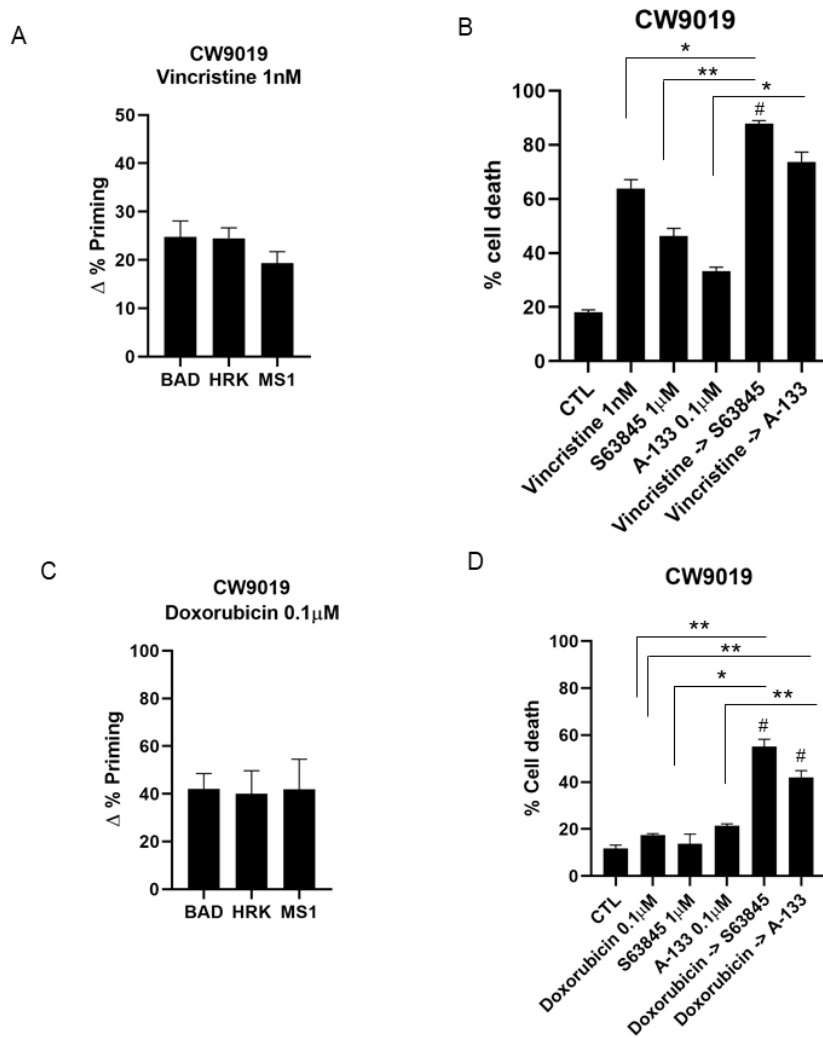
Alcon et al

Figure 2: Dynamic BH3 profiling predicts synergistic combinations with BH3 mimetics in CW9019 cell line. (A) Results from the contribution of each anti-apoptotic protein: BCL-2/BCL-xL dependence BAD peptide; BCL-xL dependence HRK peptide; and MCL-1 dependence MS1 peptide in acquiring resistance to vincristine. Results expressed as Δ% priming represents the increase in priming compared to control cells. HRK and MS1 BH3 peptides showed a significant increase, indicating BCL-xL and MCL-1 adaptation respectively (B) Cell death from Annexin V and propidium iodide staining and FACS analysis after 96 hours incubation of CW9019 cells with the single agents alone or the combination of vincristine with the corresponding BH3 mimetics S63845 and A-1331852 for 96 hours. (C) Results from the contribution of each anti-apoptotic protein. HRK and MS1 BH3 peptides showed a significant increase in priming, indicating BCL-xL and MCL-1 adaptation respectively (D) Cell death from Annexin V and propidium iodide staining and FACS analysis after 96 hours incubation of CW9019 cells with the single agents alone or the combination of doxorubicin with the BH3 mimetics S63845 and A-133. Values indicate mean values ± SEM. ** p< 0.01, * p<0.05 compared to single agents and # indicates CI<1. All experiments were performed at least three times.

Alcon et al

Vincristine induces BID sequestering by MCL-1 as a drug-induced resistance mechanism

In order to deeply study the molecular mechanism by which cells acquire resistance to vincristine and to understand why its metronomic combination with S63845 is highly effective *in vitro* we immunoprecipitated MCL-1 from CW9019 control cell lysates and CW9019 cells treated with vincristine for 36 hours (Figure 3B). MCL-1 could bind to BID preventing then the activation of BAX and BAK and therefore inhibiting cytochrome c release from the mitochondria[33]. We wanted to explore this molecular interaction as a possible mechanism to explain drug-acquired resistance to vincristine through MCL-1. We efficiently immunoprecipitated MCL-1 as we could observe a significant protein decrease in the lysate unbound fraction (Figure 3A), but a good detection in the pulled down control and treated samples compared to the Rabbit IgG negative control condition (Figure 3C). When we checked for BID co-immunoprecipitation, we observed that 36 hours after treatment with vincristine, there was a two-fold increase in MCL-1 and BID binding compared to the control (Figure 3C), leading to apoptosis protection, which explains why the sequential combination of vincristine and S63845 is effective for RMS.
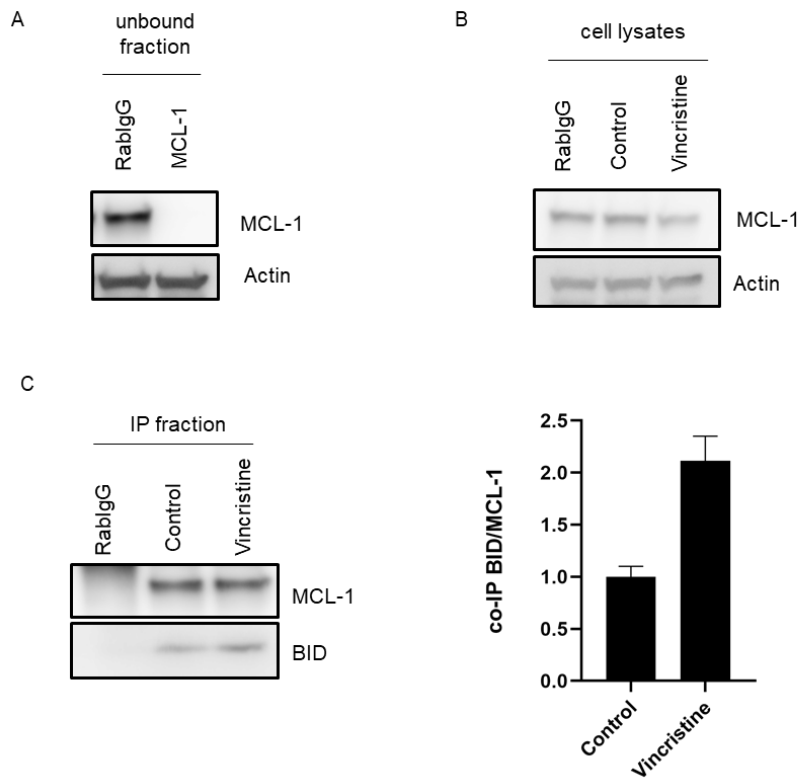
Figure 3: Vincristine induces resistance in RMS cells through BID inhibition by MCL-1. *(A) Western blot results of the unbound fraction after MCL-1 immunoprecipitation. High efficiency of MCL-1 immunoprecipitation compared to Rabbit IgG control antibody. (B) Western blot results showing MCL-1 levels in CW9019 cell lysates (incubated with vincristine or DMSO for 36 hours) before performing the immunoprecipitation. (C) Left panel: Western blot results of the co-immunoprecipitation between MCL-1 and BID. Right panel: Quantification of the optical density of each protein and represented as binding ratio between BID and MCL-1. Results expressed as fold increase represents the increase in optical density after vincristine treatment compared to control cells. Values indicate mean values ± SEM from at least three independent experiments.*

Effective therapeutic combination *in vivo* of vincristine with the MCL-1 inhibitor S63845

Patient-derived xenografts (PDXs) are advantageous in pre-clinical research as they recapitulate the therapeutic patients' outcome[22]. After identifying different effective combinations *in vitro* using cell lines, we analyzed tumors from RMS PDX models. After disaggregating the tumors to obtain a single-cell suspension, we performed DBP analyses to evaluate different therapies' effectiveness and possible anti-apoptotic adaptations. We focused on chemotherapeutic agents, particularly on vincristine as it is already utilized in the clinic to treat RMS and we found promising preliminary results *in vitro* in combination with S63845

11

Alcon et al

(Figure 1). When we analyzed a RMS PDX, we detected an increase in Δ% priming after incubating tumor cells with vincristine (Figure 4A), but not with cyclophosphamide or etoposide (Supplementary Figure 2A) as we previously observed in CW9019, RD and RH4 cell lines (Figure 1). Vincristine cytotoxicity as single agent was also predicted by DBP for this RMS PDX and reduced the tumor volume after 21 days of treatment (Figure 4C). Furthermore, we identified an anti-apoptotic adaptation mediated by MCL-1 (Figure 4B), that could diminish the efficacy of this chemotherapeutic agent, as previously observed *in vitro*. To confirm these results, we treated PDX mice with the MCL-1 inhibitor S63845 as a single agent, or right after vincristine treatment as described in materials and methods, to overcome apoptotic resistance. Surprisingly, we detected that sequentially combining vincristine and S63845 was significantly more effective than single agents and promoted tumor reduction *in vivo* (Figure 4C and Supplementary Figure 2C). Moreover, we could also observe an increase in Δ% priming after incubating tumor cells with other treatments such as S63845, ABT199 and SP2509 (Supplementary Figure 2A) and we further identified possible anti-apoptotic adaptations to those treatments by BCL-xL and MCL-1 (Supplementary Figure 2B) that we will further explore. Overall, these results demonstrate that DBP can be used to design more effective therapeutic strategies to overcome resistance and stop cancer progression.
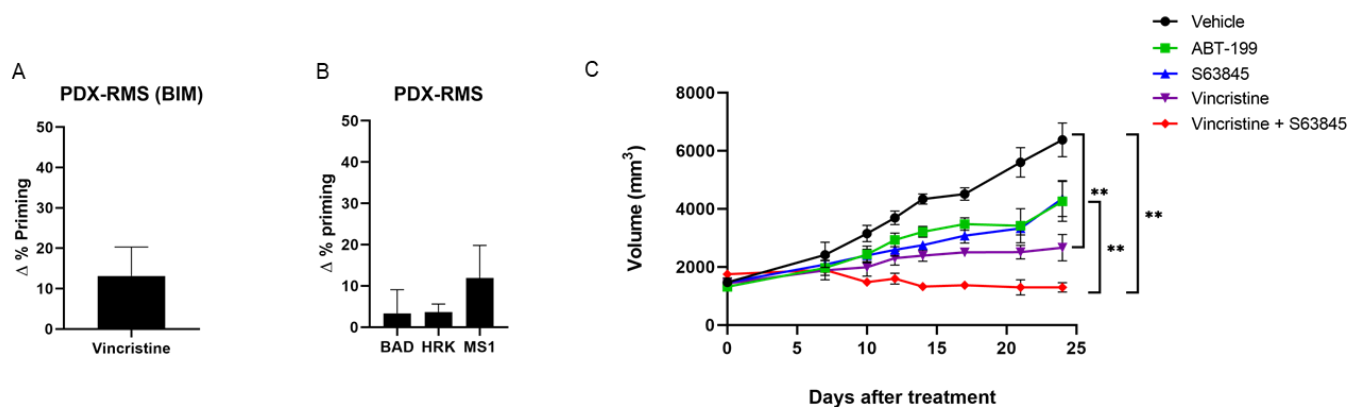
12

Alcon et al

Figure 4: Sequential treatment of vincristine and S63845 stops tumor progression in a PDX model of RMS. *(A) DBP results of PDX cells from RMS cancer patient showing an increase in Δ% priming after vincristine treatment. Results expressed as Δ% priming represents the increase in priming compared to control cells. n=2 (B) DBP results of PDX cells from RMS cancer patient with the sensitizer peptides. MS1 BH3 peptide showed a significant increase, indicating MCL-1 adaptation. n=2 (C) Tumor growth results after 21 days of treatment with vehicle, vincristine, the BH3 mimetics S63845 and ABT199 and the combination of vincristine and S63845. Day 0 indicates the day animals received the treatments. All values indicate mean values ± SEM. ** p< 0.01, n=3.*

Discussion

There is an urgent medical need to find more effective and less toxic treatments for RMS patients, since recurrent RMS has a very poor prognosis and the overall survival after relapse is very low[28]. There is a growing evidence that the BCL-2 family of proteins (particularly the anti-apoptotic members) may mediate drug resistance in cancer cells promoting patients' disease progression[7,8]. Therefore, it is key to predict these acquired pro-survival mechanisms and overcome them with anti-apoptotic inhibitors like BH3 mimetics. As we mentioned above, dynamic BH3 profiling (DBP), beyond measuring a given treatment effectiveness to engage apoptosis, can also detect anti-apoptotic adaptations derived from therapy that ensure cancer survival[13], and guide BH3 mimetics potential benefit to avoid resistance. Anti-apoptotic inhibitors such as A-1331852 (BCL-xL-selective), ABT-199 (BCL-2-selective), S63845 (MCL-1-selective) and others that are now being evaluated in clinical trials[7,27], can be used as potential targeted therapies as single agents or especially in combination with other therapies

Alcon et al

to enhance cancer cells elimination[7]. Therefore, in this study we investigated BH3 mimetics use to boost RMS sensitivity to current chemotherapy.

At present, radiotherapy, surgery and chemotherapy are the standard-of-care for RMS treatment. Regarding the latter, a three-drug combination is currently utilized: vincristine, actinomycin D and cyclophosphamide (VAC). This regimen has become the basis for RMS therapy with the incorporation of other agents such as etoposide, doxorubicin, ifosfamide, cisplatin and others for intermediate risk patients, with scarce clinical outcome improvement[34]. However, secondary effects derived from chemotherapy administration in children are severe and may include infertility, cardiomyopathy or the appearance of secondary neoplasia[34]. One explanation for these unbearable therapy-associated pediatric toxicities rely on differential apoptotic priming between young and adult tissues[21]. Traditional chemotherapy has reached an efficacy plateau in RMS making development of new therapies that increase efficacy while decreasing toxicity a clear unmet need. Thus, we sought to identify possible mechanisms of resistance to chemotherapeutic agents such as vincristine or doxorubicin by analyzing anti-apoptotic changes after treatment using DBP (Figure 2). Indeed, when we combined classical chemotherapeutic agents with BH3 mimetics we achieved a high cytotoxic effect, around 80%, while decreasing ten-fold their concentration, thus their potential secondary effects. More precisely, we identified novel synergistic combinations of vincristine with the MCL-1 inhibitor S63845, and doxorubicin with the same BH3 mimetic or the BCL-xL inhibitor A-1331852 (Figure 2). These three new combinations are synergistic as assessed by CI index (CI<1) and allowed dosing reduction[34]. These treatments have been explored in multiple adult cancers[27,35], but not in pediatric cancers where current treatments present low effectiveness especially in high risk and relapsed RMS patients[34]. Previous studies on RMS have also shown that different BH3 mimetics can potentiate chemotherapeutic treatment effectiveness[18], and increase cytotoxicity combined with an ATP-competitive mTOR inhibitor[20] or a histone deacetylase

14

inhibitor[12] which supports the idea of exploring these therapies as new approximations for treating RMS patients.

As previously mentioned, vincristine is currently used for RMS treatment[34], but we observed that cells acquire resistance through the anti-apoptotic protein MCL-1. Therefore, we focused our efforts on testing vincristine effectiveness in combination with the MCL-1 inhibitor S63845 *in vivo*. As patient-derived xenografts accurately model patients' outcome[22], we used an RMS PDX model to test the sequential combination of low dose vincristine therapy with S63845. First, we confirmed using DBP that vincristine resistance was mediated through MCL-1 in *ex vivo* PDX-isolated cancer cells (Figure 4B), correlating with our previous observations in CW9019 (Figure 2A-B). When sequentially administered a combination of vincristine followed by S63845, these PDXs showed a reduction on tumor growth with a tendency to its stabilization (Figure 4C-supplementary Figure 2C), in accordance with the high cytotoxicity observed *in vitro* (Figure 2B). To further explain this combination efficacy, we analyzed MCL-1 and NOXA expression but we could not detect significant changes on those proteins (Supplementary Figure 1 and data not shown), pointing to another anti-apoptotic mechanism driving the acquired resistance to vincristine. MCL-1 can exert its anti-apoptotic function by sequestering BID, thus inhibiting BAX and BAK activation and avoiding apoptosis[33]. There are different studies focused on trying to develop molecules that could disrupt the interaction between MCL-1 and BID and therefore restore apoptosis[36,37]. We observed an increase in MCL-1 and BID binding by co-immunoprecipitation after 36 hours treatment with vincristine compared to control (Figure 3). This increase in binding between MCL-1 and BID explains CW9019 acquired resistance to vincristine and the high efficiency of sequentially combining this chemotherapeutic agent with the MCL-1 inhibitor S63845 both *in vitro* and *in vivo*. S63845 may disrupt the interaction between MCL-1 and BID, induced as a cell defense mechanism to survive against vincristine, to engage apoptosis again in these cells,

15

Alcon et al

In summary, the work that we here present demonstrates DBP's capacity to predict days in advance the cytotoxic effect of specific treatments in RMS cells. More interestingly, it allowed to identify new mechanisms by which RMS cancer cells acquire resistance to therapy. To our knowledge, this is the first time that multiple effective sequential combinations of chemotherapeutics with BH3 mimetics are reported for RMS in the same study. Indeed, we demonstrated *in vitro* and *in vivo* the synergistic antitumor activity of the MCL-1 inhibitor S63845 when sequentially combined with vincristine. These findings, together with the current efforts on MCL-1 inhibitors, currently explored in clinical trials[38], manifest the importance of rationally combining anti-cancer agents with BH3 mimetics. These novel therapeutic strategies could improve RMS patients' treatment in the clinic, including relapsed, if guided by an effective functional predictive biomarker such as dynamic BH3 profiling.

Materials and Methods

Cell lines and treatments

RMS cell lines (CW9019, RD and RH4) were kindly provided by Dr. Oscar Martínez-Tirado and Dr. Cristina Muñoz-Pinedo from the Biomedical Research Institute from Bellvitge (IDIBELL). Cells were tested for mycoplasma and cultured in RPMI 1640 medium (Gibco, 31870) supplemented with 10% heat inactivated fetal bovine serum (Gibco, 10270), 1% of L-Glutamine (Gibco, 25030) and 1% of penicillin and streptomycin (Gibco, 15140) and maintained at 37ºC in a humidified atmosphere of 5% CO_2. Drug treatments were performed directly in the culture media at the doses and time points indicated in every single experiment.

16

Alcon et al

Dynamic BH3 Profiling

3×10^4 cells/well in a 96-well plate were used for cell lines. 25 µL of BIM BH3 peptide (final concentration of 0.01, 0.03, 0.1, 0.3, 1, 3 and 10 µM), 25 µL of BAD BH3 peptide (final concentration of 10 µM), 25 µL of HRK BH3 peptide (final concentration of 100 µM) and 25 µL of MS1 BH3 peptide [30] (final concentration of 10 µM) in MEB (150mM mannitol, 10 mM hepes-KOH pH 7.5, 150 mM KCl, 1 mM EGTA, 1 mM EDTA, 0.1% BSA, 5 mM succinate) with 0.02% digitonin were deposited per well in a 96-well plate (Corning, 3795). Single cell suspensions were stained with the viability marker Zombie Violet (BioLegend 423113) and then washed with PBS and resuspended in MEB in a final volume of 25 µL. Cell suspensions were incubated with the peptides for 1 hour following fixation with formaldehyde and staining with cytochrome c antibody (BioLegend, Alexa Fluor® 647 anti-Cytochrome c - 6H2.B4, 612310). Individual DBP analysis were performed using triplicates for DMSO, alamethecin (Enzo Life Sciences, BML-A150-0005), the different BIM BH3 concentrations used, BAD, HRK and MS1 BH3 peptides. The expressed values stand for the average of three different readings performed with a high-throughput flow cytometry SONY instrument (SONY SA3800). % priming stands for the maximum % cytochrome c released obtained from different BH3 peptide and Δ% priming stands for the maximum difference between treated cells minus non-treated cells.

Cell death analysis

Cells were stained with fluorescent conjugates of Annexin-V (BioVision, 1001) and/or propidium iodide (PI) (BioVision, 1056) and analyzed on a flow cytometry Gallios instrument (Beckman Coulter). Viable cells are Annexin-V negative and PI negative, and cell death is expressed as 100%-viable cells.

Alcon et al

Protein extraction and quantification

Proteins were extracted by lysing the cells during 30min at 4ºC using RIPA buffer (150 mM NaCl, 5 mM EDTA, 50 mM Tris-HCl pH=8, 1% Triton X-100, 0.1% SDS, EDTA-free Protease Inhibitor Cocktail) followed by a centrifugation at 16100 g for 10 min. The supernatant was stored at -20ºC for protein quantification performed using Pierce ^{TM} BCA Protein Assay Kit (ThermoFisher, 23227).

Immunoprecipitation

Cells were lysed in Immunoprecipitation buffer (150mM NaCl, 10mM Hepes, 2mM EDTA, 1% Triton, 1.5mM MgCl2, 10% glycerol, protease inhibitor from Roche) and centrifuged at 14,000 g, 15min at 4ºC. The resulting supernatants were incubated with magnetic beads (Bio-Rad, 161-4021) conjugated to rabbit anti-MCL-1 antibody (5μg, Cell Signaling, CST94296) or Rabbit IgG antibody (5μg, Cell Signaling, CST2729) at 4ºC overnight. A fraction of the supernatant (30μL) were removed and mixed with half volume of 4X SDS-PAGE sample buffer, heated at 96ºC for 5 minutes and stored at -80ºC as input fractions. After magnetization, a part of the supernatant was mixed with half volume of 4X SDS-PAGE sample buffer, heated at 96ºC for 5 minutes and stored at -80ºC as unbound fractions. The rest of the supernatant was discarded. The resulting pellet was washed and mixed with 40μL 4X SDSPAGE sample buffer and heated 10min at 70ºC to allow the dissociation between the purified target proteins and the beads-antibody complex. Finally, sample was magnetized and the supernatant was collected and stored at -80ºC as IP fractions for further western blot analysis.

Alcon et al

Immunoblotting

Proteins were separated by SDS/PAGE (Mini-Protean TGX Precast Gel 12%, Bio-Rad, 456-1045) and transferred to PVDF membranes (Amersham Hybond, 10600023). Membranes were blocked with dry milk dissolved in Tris Buffer Saline with 1% Tween 20 (TBST) for 1 hour and probed overnight at 4°C with the primary antibodies of interest directed against: rabbit anti-BCL-2 (Cell Signaling, CST4223), rabbit anti-BCL-xL (Cell Signaling, CST2764), rabbit anti-MCL-1 (Cell Signaling, CST5453), rabbit anti-NOXA (Cell Signaling), rabbit anti-BIM (Cell Signaling, CST2933), rabbit anti-Actin (Cell Signaling, CST4970) followed by Anti-rabbit IgG HRP-linked secondary antibody (Cell Signaling, CST7074) in 3% BSA in TBST for 1 hour at room temperature. Immunoblots were developed using Clarity ECL Western substrate (Bio-Rad, 1705060). When necessary, immunoblots were stripped in 0.1M glycine pH 2,5, 2% SDS for 40 minutes and washed in TBS. Bands were visualized with LAS4000 imager and ImageJ was then used to measure the integrated optical density of bands.

Animals and human tissue

Six-week-old male athymic nu/nu mice (Envigo) weighing 18–22 g were used in this study. Animals were housed in a sterile environment, in cages with autoclaved bedding, food, and water. The mice were maintained on a daily 12 hours light, 12 hours dark cycle. The patient gave written consent to participate in the study. The Institutional Ethics Committees approved the study protocol, and the animal experimental design was approved by the IDIBELL animal facility committee (AAALAC Unit1155). All experiments were performed in accordance with the guideline for Ethical Conduct in the Care and Use of Animals as stated in The International Guiding Principles for Biomedical Research Involving Animals, developed by the Council for International Organizations of Medical Sciences.

Alcon et al

Development of rhabdomyosarcoma orthoxenograft mouse model

A embryonal rhabdomyosarcoma (ERMS) orthoxenograft was generated from a small biopsy of a metastatic case taken at diagnostic from the primary tumor located in the child gluteus of a metastatic child. The primary tumor did not receive radiotherapy or chemotherapy prior to surgery. Under isoflurane anesthesia, a subcutaneous pocket was made with surgical scissors. Then, a small incision was made in the muscle and the tumor was fixed with synthetic monofilament, non-absorbable polypropylene suture (Prolene 7.0) to the muscle of the upper thigh (orthotopic implantation). After implantation, tumor formation was checked weekly by palpation. Orthotopic tumor (named RMSX1) became apparent 1–3 months after engraftment. Once orthotopic tumors had reached a volume of around 1,500 mm3, mice were sacrificed and tumors were passed to another three animal in order to obtain a sufficient quantity of tumor material. After each passage tumors were frozen, paraffin-embedded, and cryopreserved in (10% DMSO + 90% Fetal Bovine Serum (FBS) (non-inactivated) to provide a source of viable tissue for future experiments.

Drug treatment in embryonal rhabdomyosarcoma RMSX1 orthoxenograft tumor model

The MPNST orthoxenograft procedure was approved by the campus Animal Ethics Committee and complied with AAALAC (Association for Assessment and Accreditation of Laboratory Animal Care International) procedures. A mouse harboring RMSX1 tumor orthotopically growing (at passage#2) was sacrificed, tumors were harvested and cut into small fragments 4x 4 mm^3, and the tumor fragments were grafted in 20 young mice. When tumors reached a homogeneous size (1200 to 1500 mm^3) mice were randomly allocated into the different treatment groups (n=4/group): i) Placebo; ii) ABT199 (100 mg/kg); iii) vincristine (1 mg/kg); iv) S63845 (20 mg/kg); and v) combined vincristine (1 mg/kg) plus S63845 (20 mg/kg). Vincristine was intravenous administrated by tail vein injection (i.v)

20

Alcon et al

once per week for 3 consecutive weeks (days 0, 7, and 14). ABT199 was daily administered (q.d) by oral gavage (p.o) for 21 days and S63845 was i.v administered three consecutive days per week for 2 weeks. All the animals/groups were sacrificed at day 21. To minimize in combined treatments the risk to develop drug induced toxicity drugs were administered spaced in time. Vincristine was administered first and S63845 2 hours later. Vincristine from Eli Lilly (1 mg/ml) was purchased at the hospital pharmacy of Catalan Institute of Oncology (ICO) and diluted in saline before use. ABT199 and S63845 were purchased at Selleckchem. ABT199 was diluted in 10% Ethanol/30% PEG 400/60% Phosal 50 PG (v/v/v) while S63845 was diluted in 10% DMSO/40% PEG300/5% Tween 80/Saline. After treatment initiation, tumors were measured using a caliper every 2–3 days and tumor volume was calculated using the formula $v = (w2\ l/2)$, where l is the longest diameter and w the width. At sacrifice, tumor was dissected out and weighed. Representative fragments were either frozen in nitrogen or fixed and then processed for paraffin embedding.

PDX cell isolation

Primary tumors from PDX animals were exposed to an enzymatic digestion after, mechanical disaggregation, in 2.5 mL of DMEM media with 125 units of DNAse I (Sigma-Aldrich, DN25), 100 units of Hyaluronidase (Sigma-Aldrich, H3506) and 300 units of collagenase IV (Gibco, 17104–019). The tissue suspension was processed using gentleMACS Dissociator (Miltenyl Biotec) using the hTUMOR 1 program. The suspension was incubated at 37°C for 30 min in constant agitation. After the program hTUMOR 1 was ran again and repeated the 30 min incubation. We filtered the suspension 70 micron filter into a 50 mL conical and cells were spinned down $500 \times g$ for 5 min. To lyse the residual red blood cells, 100 µL of ice cold water was added for 15 s and then diluted to 50 mL with PBS, then spin cells down again. Cells were

Alcon et al

finally resuspended in RPMI media, counted by trypan blue exclusion and plated in a 12-well plate, 3 x 10^4 cells/well and treated with DMSO or vincristine 1nM. After a 16 hours incubation at 37°C in a humidified atmosphere of 5% CO_2. Dynamic BH3 profiling analyses were then performed.

Statistical analysis

Statistical analysis P values 0.05 were considered as statistically significant and results were analyzed using Student's t-tail test. SEM stands for Standard Error of the Mean. For ROC curve analysis cell lines were considered responsive to treatment when Δ% cell death > 20 %. Drug synergies were established based on the Bliss Independent model as previously described [31]. Combinatorial index (CI) was calculated CI= $((D_A+D_B)-(D_A*D_B))/D_{AB}$, where D represents cell death of compound A or B or the combination of both. Only the combination of drugs with a CI<1 were considered synergies. GraphPad Prism8 was used to generate the graphs and to perform the statistical analysis.

Author contributions C. Alcon performed and analyzed all the *in vitro* experiments. C. Alcon performed the PDX tumors disaggregation and their analysis. A. Villanueva and A. Soriano performed and analyzed the *in vivo* experiments. G. Guillén and J. Roma provided the tumors

22

for the *in vivo* experiments. E. Prada and J. Mora provided some reagents used in the article. C. Alcon and J. Montero wrote the manuscript. J. Montero supervised the work.

Compliance with ethical standards

Conflict of interest J. Montero was a paid consultant for Oncoheroes Biosciences and Vivid Biosciences and is an unpaid board member for The Society for Functional Precision Medicine. A. Villanueva is cofounder of the Spin-off of Xenopat S.L and has ownership interests. No potential conflicts of interest were disclosed by the other authors.

References

1.   De Giovanni C, Landuzzi L, Nicoletti G, Lollini PL, Nanni P. Molecular and cellular biology of rhabdomyosarcoma. *Futur Oncol*. 2009;5(9):1449-1475. doi:10.2217/fon.09.97

2.   Sun X, Guo W, Shen JK, Mankin HJ, Hornicek FJ, Duan Z. Rhabdomyosarcoma: Advances in molecular and cellular biology. *Sarcoma*. 2015;2015. doi:10.1155/2015/232010

3.   Hoang NT, Acevedo LA, Mann MJ, Tolani B. A review of soft-tissue sarcomas: Translation of biological advances into treatment measures. *Cancer Manag Res*. 2018;10:1089-1114. doi:10.2147/CMAR.S159641

4.   Belyea B, Kephart JG, Blum J, Kirsch DG, Linardic CM. Embryonic signaling pathways and rhabdomyosarcoma: Contributions to cancer development and opportunities for therapeutic targeting. *Sarcoma*. 2012;2012. doi:10.1155/2012/406239

5.   Hawkins DS, Gupta AA, Rudzinski ER. What is new in the biology and treatment of pediatric rhabdomyosarcoma? *Curr Opin Pediatr*. 2014;26(1):50-56. doi:10.1097/MOP.0000000000000041

Alcon et al

6.   Brunelle JK, Letai A. Control of mitochondrial apoptosis by the Bcl-2 family. *J Cell Sci*. 2009;122(4):437-441. doi:10.1242/jcs.031682

7.   Montero J, Letai A. Why do BCL-2 inhibitorswork and where should we use them in the clinic? *Cell Death Differ*. 2018;25(1):56-64. doi:10.1038/cdd.2017.183

8.   Frenzel A, Grespi F, Chmelewskij W, Villunger A. Europe PMC Funders Group Bcl2 family proteins in carcinogenesis and the treatment of cancer. 2012;14(4):584-596. doi:10.1007/s10495-008-0300-z.Bcl2

9.   Place AE, Goldsmith K, Bourquin JP, et al. Accelerating drug development in pediatric cancer: A novel Phase i study design of venetoclax in relapsed/refractory malignancies. *Futur Oncol*. 2018;14(21):2115-2129. doi:10.2217/fon-2018-0121

10.   Armistead PM, Salganick J, Roh JS, et al. Expression of receptor tyrosine kinases and apoptotic molecules in rhabdomyosarcoma: Correlation with overall survival in 105 patients. *Cancer*. 2007;110(10):2293-2303. doi:10.1002/cncr.23038

11.   Pazzaglia L, Chiechi A, Conti A, et al. Genetic and molecular alterations in rhabdomyosarcoma: mRNA overexpression of MCL1 and MAP2K4 genes. *Histol Histopathol*. 2009;24(1):61-67. doi:10.14670/HH-24.61

12.   Heinicke U, Haydn T, Kehr S, Vogler M, Fulda S. BCL-2 selective inhibitor ABT-199 primes rhabdomyosarcoma cells to histone deacetylase inhibitor-induced apoptosis. *Oncogene*. 2018;37(39):5325-5339. doi:10.1038/s41388-018-0212-5

13.   Montero J, Letai A. Dynamic BH3 profiling-poking cancer cells with a stick. *Mol Cell Oncol*. 2016;3(3):1-3. doi:10.1080/23723556.2015.1040144

14.   Montero J, Stephansky J, Cai T, et al. Blastic plasmacytoid dendritic cell neoplasm is dependent on BCL2 and sensitive to venetoclax. *Cancer Discov*. 2017;7(2):156-164. doi:10.1158/2159-8290.CD-16-0999

15.   Deng J, Isik E, Fernandes SM, Brown JR, Letai A, Davids MS. Bruton's tyrosine kinase

Alcon et al

inhibition increases BCL-2 dependence and enhances sensitivity to venetoclax in chronic lymphocytic leukemia. *Leukemia*. 2017;31(10):2075-2084. doi:10.1038/leu.2017.32

16.   Townsend EC, Murakami MA, Christodoulou A, et al. The Public Repository of Xenografts Enables Discovery and Randomized Phase II-like Trials in Mice. *Cancer Cell*. 2016;29(4):574-586. doi:10.1016/j.ccell.2016.03.008

17.   Wu SC, Li LS, Kopp N, et al. Activity of the Type II JAK2 Inhibitor CHZ868 in B Cell Acute Lymphoblastic Leukemia. *Cancer Cell*. 2015;28(1):29-41. doi:10.1016/j.ccell.2015.06.005

18.   Meister MT, Boedicker C, Klingebiel T, Fulda S. Hedgehog signaling negatively co-regulates BH3-only protein Noxa and TAp73 in TP53-mutated cells. *Cancer Lett*. 2018;429:19-28. doi:10.1016/j.canlet.2018.04.025

19.   Faqar-Uz-Zaman SF, Heinicke U, Meister MT, Vogler M, Fulda S. BCL-xL-selective BH3 mimetic sensitizes rhabdomyosarcoma cells to chemotherapeutics by activation of the mitochondrial pathway of apoptosis. *Cancer Lett*. 2018;412(September):131-142. doi:10.1016/j.canlet.2017.09.025

20.   Preuss E, Hugle M, Reimann R, Schlecht M, Fulda S. Pan-Mammalian Target of Rapamycin (mTOR) Inhibitor AZD8055 Primes Rhabdomyosarcoma Cells for ABT-737- induced Apoptosis by Down-regulating Mcl-1 Protein. *J Biol Chem*. 2013;288(49):35287-35296. doi:10.1074/jbc.M113.495986

21.   Sarosiek KA, Fraser C, Muthalagu N, et al. Developmental Regulation of Mitochondrial Apoptosis by c-Myc Governs Age- and Tissue-Specific Sensitivity to Cancer Therapeutics. *Cancer Cell*. 2017;31(1):142-156. doi:10.1016/j.ccell.2016.11.011

22.   Adamson PC. Improving the outcome for children with cancer: Development of targeted new agents. *CA Cancer J Clin*. 2015;65(3):212-220. doi:10.3322/caac.21273

Alcon et al

23.   Melguizo C, Prados J, Rama AR, et al. Multidrug resistance and rhabdomyosarcoma (review). *Oncol Rep*. 2011;26(4):755-761. doi:10.3892/or.2011.1347

24.   Skapek SX, Ferrari A, Gupta AA, et al. Rhabdomyosarcoma. *Nat Rev Dis Prim*. 2019;5(1):14-16. doi:10.1038/s41572-018-0051-2

25.   Foucquier J, Guedj M. Analysis of drug combinations: current methodological landscape. *Pharmacol Res Perspect*. 2015;3(3). doi:10.1002/prp2.149

26.   Cree IA, Charlton P. Molecular chess? Hallmarks of anti-cancer drug resistance. *BMC Cancer*. 2017;17(1):1-8. doi:10.1186/s12885-016-2999-1

27.   Montero J, Gstalder C, Kim DJ, et al. Destabilization of NOXA mRNA as a common resistance mechanism to targeted therapies. *Nat Commun*. 2019;10(1). doi:10.1038/s41467-019-12477-y

28.   Montero J, Sarosiek KA, Deangelo JD, et al. Drug-Induced death signaling strategy rapidly predicts cancer response to chemotherapy. *Cell*. 2015;160(5):977-989. doi:10.1016/j.cell.2015.01.042

29.   Ryan J, Montero J, Rocco J, Letai A. IBH3: Simple, fixable BH3 profiling to determine apoptotic priming in primary tissue by flow cytometry. *Biol Chem*. 2016;397(7):671-678. doi:10.1515/hsz-2016-0107

30.   Foight GW, Ryan JA, Gullá S V., Letai A, Keating AE. Designed BH3 peptides with high affinity and specificity for targeting Mcl-1 in cells. *ACS Chem Biol*. 2014;9(9):1962-1968. doi:10.1021/cb500340w

31.   Manstein V, Yang C, Richter D, Delis N, Vafaizadeh V, Groner B. Resistance of Cancer Cells to Targeted Therapies Through the Activation of Compensating Signaling Loops. *Curr Signal Transduct Ther*. 2014;8(3):193-202. doi:10.2174/1574362409666140206221931

32.   Fitzgerald JB, Schoeberl B, Nielsen UB, Sorger PK. Systems biology and combination

therapy in the quest for clinical efficacy. *Nat Chem Biol*. 2006;2(9):458-466. doi:10.1038/nchembio817

33. Clohessy JG, Zhuang J, De Boer J, Gil-Gómez G, Brady HJM. Mcl-1 interacts with truncated bid and inhibits its induction of cytochrome c release and its role in receptor-mediated apoptosis. *J Biol Chem*. 2006;281(9):5750-5759. doi:10.1074/jbc.M505688200

34. Huh W, Egas Bejar D. Rhabdomyosarcoma in adolescent and young adult patients: current perspectives. *Adolesc Health Med Ther*. 2014:115. doi:10.2147/ahmt.s44582

35. Pallis M, Burrows F, Ryan J, et al. Complementary dynamic BH3 profiles predict co-operativity between the multi-kinase inhibitor TG02 and the BH3 mimetic ABT-199 in acute myeloid leukaemia cells. *Oncotarget*. 2017;8(10):16220-16232. doi:10.18632/oncotarget.8742

36. Apel C, Gény C, Dumontet V, et al. Endiandric acid analogues from Beilschmiedia ferruginea as dual inhibitors of Bcl-xL/Bak and Mcl-1/bid interactions. *J Nat Prod*. 2014;77(6):1430-1437. doi:10.1021/np500170v

37. Azmi MN, Péresse T, Remeur C, et al. Kingianins O-Q: Pentacyclic polyketides from Endiandra kingiana as inhibitor of Mcl-1/Bid interaction. *Fitoterapia*. 2016;109:190-195. doi:10.1016/j.fitote.2016.01.004

38. Hird AW, Tron AE. Recent advances in the development of Mcl-1 inhibitors for cancer therapy. *Pharmacol Ther*. 2019;198:59-67. doi:10.1016/j.pharmthera.2019.02.007